Proceedings of the
47th IEEE Conference on Decision and Control
Cancun, Mexico, Dec. 9-11, 2008

Influence of tire damping on the ride performance potential of quarter-car active suspensions

Semiha Türkay and Hüseyin Akçay

Abstract— **In this paper, performance limitations are studied for a quarter-car active suspension system excited by sinusoidal or random road disturbances. It is demonstrated that the influence of tire damping on the closed-loop performance of the active suspension system can be significant.**

I. INTRODUCTION

Active and semi-active control of vehicle suspensions have been the subject of considerable investigation since the late 1960s; see, for example [1], [2] and the references therein. Constraints and trade-offs on achievable performances have been studied in [3], [4], [5], [6], [7], [8].

In [6], for a quarter-car model of an automotive suspension a *complete* set of constraints on several transfer functions of interest from the road and the load disturbances were determined by making use of the *factorization* approach to feedback stability and the Youla *parameterization* of stabilizing controllers. These constraints typically arise in the form of finite and nonzero invariant frequency points and the growth restrictions on the frequency responses and their derivatives at zero and infinite frequencies.

In most works, tire damping is ignored when modeling automotive active suspension systems. This is partly due to the fact that tire damping is difficult to estimate. The tire damping by itself has little influence on the wheel-hop vibration since this mode is mainly damped by the shock absorber. The ignorance of damping in tire models compelled misleading conclusions that at the wheel-hop frequency, motions of the sprung and unsprung masses are uncoupled, and the vertical acceleration of the sprung mass will be unaffected [3], [4], [6]. It is pointed out in [9] that by taking tire damping to be small but nonzero, the motions of the sprung and unsprung masses are coupled at all frequencies, and control forces can be used to reduce the sprung mass vertical acceleration at the wheel-hop frequency. The effect of introducing tire damping can be quite large.

The study of the constraints on the achievable performance has remained largely restricted to point-wise constraints in the frequency domain while ride comfort and safety criteria are mostly expressed in terms of the root–mean–square (rms) values of the sprung mass vertical acceleration, the suspension travel, and the tire deflection frequency responses. It is generally agreed that typical road surfaces may be considered as realizations of homogeneous and isotropic two-dimensional Gaussian random processes and these assumptions make it possible to completely describe a road profile by a single power spectral density evaluated from any longitidunal track [10]. Then, the spectral description of the road, together with a knowledge of traversal velocity and of the dynamic properties of the vehicle, provide a response analysis which will describe the response of the vehicle expressed in terms of displacement, acceleration, or stress.

This paper is structured as follows. In § II, a two-degree-of quarter car model is reviewed. In § III, all achievable transfer functions from the road disturbance to the sprung mass vertical acceleration, the suspension travel, and the tire deflection are parametrized. A complete set of constraints are derived in § IV. In § V, the effect of tire damping on the controller design is illustrated by a numerical example. In § VI, all achievable rms responses of the quarter-car model to white-noise velocity road inputs are parameterized and an optimization problem that aims to minimize weighted sums of the rms values of the outputs with respect to the class of all stabilizing controllers is formulated. Solution of this problem is obtained in § VII for a range of tire damping coefficient. The paper is concluded by § VIII.

II. THE QUARTER-CAR MODEL

A two-degree-of-freedom quarter-car model is shown in Fig. 1. In this model, the sprung and unsprung masses are denoted, respectively, by m_{s} and m_{u}. The suspension system is represented by a linear spring of stiffness k_{s} and a linear damper with a damping rate c_{s}. The tire is modeled by a linear spring of stiffness k_{t} and a linear damper with a damping rate c_{t}. The parameter values, except c_{t}, chosen for this study are shown in Table 1.

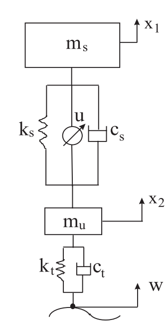

Fig. 1. The quarter-car model of the vehicle.

Assuming that the tire behaves as a point-contact follower that is in contact with the road at all times, the equations of

Department of Electrical and Electronics Engineering, Anadolu University, 26470 Eskişehir, Turkey. This work was supported in part by the Scientific & Technological Research Council of Turkey under Grant 106E108. E-mails: {semihaturkay,huakcay}@anadolu.edu.tr.

TABLE I

THE VEHICLE SYSTEM PARAMETERS FOR THE QUARTER-CAR MODEL.

Sprung mass	m_s	240 kg
Unsprung mass	m_u	36 kg
Damping coefficient	c_s	980 Ns/m
Secondary suspension stiffness	k_s	16,000 N/m
Primary suspension stiffness	k_t	160,000 N/m

motion take the form

$$\begin{aligned} m_{\rm s}\ddot{\mathbf{x}}_1 &= -k_{\rm s}(\mathbf{x}_1-\mathbf{x}_2)-c_{\rm s}(\dot{\mathbf{x}}_1-\dot{\mathbf{x}}_2)-u, \\ m_{\rm u}\ddot{\mathbf{x}}_2 &= k_{\rm s}(\mathbf{x}_1-\mathbf{x}_2)+c_{\rm s}(\dot{\mathbf{x}}_1-\dot{\mathbf{x}}_2) \\ &\quad +u-k_{\rm t}(\mathbf{x}_2-w)-c_{\rm t}(\dot{\mathbf{x}}_2-\dot{w}) \end{aligned} \tag{1}$$

where $\mathbf{x}_1$ and $\mathbf{x}_2$ are respectively the displacements of the sprung and unsprung masses, and w is the road unevenness. The variables $\mathbf{x}_1, \mathbf{x}_2$, and w are measured with respect to an inertial frame, and the control input u is a force.

The objective of this paper is to study the performance limits of an actively controlled vehicle imposed by the road surface unevenness. The vehicle response variables that need to be examined are the vertical acceleration of the sprung mass as an indicator of the vibration isolation, the suspension travel as a measure of the rattling space, and the tire deflection as an indicator of the road-holding characteristic of the vehicle. These variables, denoted respectively by $\mathbf{z}_1, \mathbf{z}_2$, and $\mathbf{z}_3$, can be written in terms of the state variables $\mathbf{x}_1, \mathbf{x}_2$, their derivatives, and the exogenous input w as follows:

$$\mathbf{z}_1 = \ddot{\mathbf{x}}_1, \tag{2}$$

$$\mathbf{z}_2 = \mathbf{x}_1-\mathbf{x}_2, \tag{3}$$

$$\mathbf{z}_3 = \mathbf{x}_2-w. \tag{4}$$

Passenger comfort requires $\mathbf{z}_1$ to be as small as possible while compactness of rattle space, good handling characteristics, and improved road-holding quality require $\mathbf{z}_2$ and $\mathbf{z}_3$ be kept as small as possible.

It is a well-known fact [5] that these objectives can not be met simultaneously with a passive suspension system. The conflicting three goals can be attained up to a certain level by replacing passive suspension system with an active or semi-active suspension system [1], [2], [6].

III. FACTORIZATION APPROACH TO FEEDBACK STABILITY

Let $\mathbf{Z}(s)$, $U(s)$, and $W(s)$ denote respectively the Laplace transforms of the signals $\mathbf{z}(t)=[\mathbf{z}_1(t)\ \mathbf{z}_2(t)\ \mathbf{z}_3(t)]^T$, $u(t)$ and $w(t)$, where for a given vector $\mathbf{b}$, $\mathbf{b}^T$ denotes the transpose of $\mathbf{b}$. From (1)–(4),

$$\mathbf{Z}(s)=\mathbf{G}_{11}(s)W(s)+\mathbf{G}_{12}(s)U(s)$$

where

$$\mathbf{G}_{11}(s) = \frac{1}{\Delta(s)}\begin{bmatrix} s^2(c_{\rm s}s+k_{\rm s})(c_{\rm t}s+k_{\rm t}) \\ -m_{\rm s}s^2(c_{\rm t}s+k_{\rm t}) \\ -s^2[m_{\rm s}m_{\rm u}s^2+(m_{\rm s}+m_{\rm u})c_{\rm s}s \\ \quad +(m_{\rm s}+m_{\rm u})k_{\rm s}] \end{bmatrix},$$

$$\mathbf{G}_{12}(s) = \frac{1}{\Delta(s)}\begin{bmatrix} -s^2(m_{\rm u}s^2+c_{\rm t}s+k_{\rm t}) \\ -[(m_{\rm s}+m_{\rm u})s^2+c_{\rm t}s+k_{\rm t}] \\ m_{\rm s}s^2 \end{bmatrix},$$

and

$$\begin{aligned} \Delta(s) &= m_{\rm s}m_{\rm u}s^4+[(m_{\rm s}+m_{\rm u})c_{\rm s}+m_{\rm s}c_{\rm t}]s^3 \\ &\quad +[(m_{\rm s}+m_{\rm u})k_{\rm s}+m_{\rm s}k_{\rm t}+c_{\rm s}c_{\rm t}]s^2 \\ &\quad +(c_{\rm s}k_{\rm t}+c_{\rm t}k_{\rm s})s+k_{\rm s}k_{\rm t}. \end{aligned}$$

For the design of a feedback law, we consider the suspension travel measurement:

$$\mathbf{y} = \mathbf{x}_1-\mathbf{x}_2.$$

From (1)–(4),

$$\mathbf{Y}(s)=\mathbf{G}_{21}(s)W(s)+\mathbf{G}_{22}(s)U(s)$$

where

$$\mathbf{G}_{21}(s) = -\frac{m_{\rm s}s^2(c_{\rm t}s+k_{\rm t})}{\Delta(s)},$$

$$\mathbf{G}_{22}(s) = -\frac{(m_{\rm s}+m_{\rm u})s^2+c_{\rm t}s+k_{\rm t}}{\Delta(s)}.$$

Hence, the generalized plant defined by

$$\mathbf{G}(s)=\left[\begin{array}{c|c} \mathbf{G}_{11} & \mathbf{G}_{12} \\ \hline \mathbf{G}_{21} & \mathbf{G}_{22} \end{array}\right]$$

maps the pair of inputs $[w\ u]^T$ to the pair of outputs $[\mathbf{z}^T\ \mathbf{y}]^T$.

Now, let $\mathbf{K}(s)$ denote the transfer function of the controller with input $\mathbf{y}$ and the output u. The feedback configuration is shown in Fig. 2. The stabilization problem is to find a proper feedback transfer function $\mathbf{K}$ such that the closed-loop system in Fig. 2 is *internally stable*. Assuming that $\mathbf{G}$ and $\mathbf{G}_{22}$ share the same unstable poles, it is a well-known fact that $\mathbf{K}$ internally stabilizes $\mathbf{G}$ if and only if $\mathbf{K}$ internally stabilizes $\mathbf{G}_{22}$.

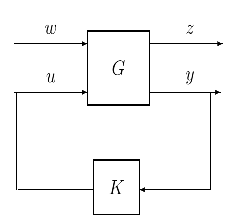

Fig. 2. Standard block diagram.

Assuming that $\mathbf{G}_{22}$ is internally stabilizable, the set of all compensators which stabilize $\mathbf{G}$ can be parametrized in terms of a *coprime factorization* of $\mathbf{G}_{22}$. This parametrization is called the Youla parametrization. The Youla parametrization of all stabilizing controllers takes the form:

$$\begin{aligned} \mathbf{K} &= (\mathbf{Y}-\mathbf{MQ})(\mathbf{X}-\mathbf{NQ})^{-1},\ \mathbf{Q}\in\mathscr{RH}_\infty, \\ &\quad \det(\mathbf{I}-\mathbf{X}^{-1}\mathbf{NQ})(\infty)\neq 0 \end{aligned} \tag{5}$$

where $\mathscr{RH}_\infty$ denotes the set of stable real-rational transfer functions.

With this parametrization, the transfer matrix from w to $\mathbf{z}$ denoted by $\mathbf{T}_{\mathbf{z}\mathrm{w}}(s)$ takes a particularly convenient form:

$$\mathbf{T}_{\mathbf{z}\mathrm{w}} = \mathbf{G}_{11} + \mathbf{G}_{12}(\mathbf{Y} - \mathbf{MQ})\widetilde{\mathbf{M}}\mathbf{G}_{21}. \qquad (6)$$

As $\mathbf{Q}$ varies over $\mathscr{RH}_\infty$, (6) parametrizes all achievable transfer matrices.

IV. ACHIEVABLE PERFORMANCE FOR QUARTER-CAR MODEL

In the design of active suspension systems, it is desirable to keep the road response amplitudes $|\mathbf{T}_{\mathbf{z}_k\mathrm{w}}(\mathrm{j}\omega)|$, $k = 1,2,3$ as small as possible, at least in the frequency range of interest.

By using different measurements for feedback, constraints on the closed-loop transfer functions $\mathbf{T}_{\mathbf{z}_k\mathrm{w}}$ were derived in [8]. In the following, a subset of these results are presented.

Proposition 4.1: Consider the quarter-car model (1) with $k_\mathrm{s}, c_\mathrm{s}, c_\mathrm{t} > 0$. Let $\mathbf{H}_1$ be an arbitrary function in $\mathscr{RH}_\infty$. Then, $\mathbf{H}_1 = \mathbf{T}_{\mathbf{z}_1\mathrm{w}}$ for some stabilizing control law if and only if:

1) $\mathbf{H}_1(s) = \dfrac{c_\mathrm{s}c_\mathrm{t}}{m_\mathrm{s}m_\mathrm{u}} + O(s^{-1})$,

2) $\mathbf{H}_1(0) = \mathbf{H}_1^{(1)}(0) = \mathbf{H}_1^{(3)}(0) = 0, \qquad \mathbf{H}_1^{(2)}(0) = 2.$

Now, assume that $c_\mathrm{t} = 0$ and $k_\mathrm{s}, c_\mathrm{s} > 0$. Two new constraints arise at the frequencies:

$$\omega_1 = \sqrt{\frac{k_\mathrm{t}}{m_\mathrm{s} + m_\mathrm{u}}}, \qquad \omega_2 = \sqrt{\frac{k_\mathrm{t}}{m_\mathrm{u}}} \qquad (7)$$

which have already been observed in [4], [6]. The results for this case are captured in the following.

Proposition 4.2: Consider the quarter-car model (1) with $k_\mathrm{s}, c_\mathrm{s} > 0$, and $c_\mathrm{t} = 0$. Let $\mathbf{H}_1$ be any function in $\mathscr{RH}_\infty$. Then, $\mathbf{H}_1 = \mathbf{T}_{\mathbf{z}_1\mathrm{w}}$ for some stabilizing control law if and only if:

1) $\mathbf{H}_1(s) = \dfrac{k_\mathrm{t}c_\mathrm{s}}{m_\mathrm{s}m_\mathrm{u}} s^{-1} + O(s^{-2})$,

2) $\mathbf{H}_1(0) = \mathbf{H}_1^{(1)}(0) = \mathbf{H}_1^{(3)}(0) = 0, \qquad \mathbf{H}_1^{(2)}(0) = 2,$

3) $\mathbf{H}_1(\mathrm{j}\omega_2) = -(\mathrm{j}\omega_2)^2 \dfrac{m_\mathrm{u}}{m_\mathrm{s}}$.

Similar results can be obtained for $\mathbf{H}_2$ and $\mathbf{H}_3$ corresponding to $\mathbf{T}_{z_2\mathrm{w}}$ and $\mathbf{T}_{z_3\mathrm{w}}$. No matter how small, observe that tire damping couples the wheel-hop and the heave modes. This coupling eliminates the constraints of the conventional quarter-car model, which neglects tire damping at the *so-called* invariant frequencies ω_1 and ω_2. As will be seen in the next section, tire damping improves ride comfort without sacrificing road holding.

V. ACTIVE CONTROL OF THE QUARTER-CAR MODEL

The purpose of this section is to illustrate the effect of tire damping on the controller design for the quarter-car model. The vehicle is assumed to traverse a random road profile with a constant forward velocity v. For simplicity, the random process V_i is modeled as

$$V_i = \dot{w} = 2\pi n_0 \sqrt{\kappa v}\, \eta(t), \qquad t \geq 0 \qquad (8)$$

where $\eta(t)$ is a zero-mean white-noise process with an auto covariance function $R_\eta(\tau) = \delta(t)$; $\kappa = 0,76 \times 10^{-5}$ and $n_0 = 0.15708$ are the road roughness parameters for the road data in [8]; and $\delta(t)$ is the unit-impulse function.

Notice the relation $\mathbf{T}_{\mathbf{z}\mathrm{V_i}} = s^{-1}\mathbf{T}_{\mathbf{z}\mathrm{w}}$. Thus, the Q-parametrization of $\mathbf{T}_{\mathbf{z}\mathrm{V_i}}$ can be deduced from the Q-parametrization of $\mathbf{T}_{\mathbf{z}\mathrm{w}}$. In particular, they share the same invariant frequencies ω_1 and ω_2.

The controllers are designed using the Linear-Quadratic-Gaussian (LQG) design methodology. In Fig. 3, the frequency response magnitudes of the passive and the active suspensions using either suspension travel measurement or both the acceleration and the suspension travel measurements are plotted for the parameter values in Table 1, and $c_\mathrm{t} = 0$. The rms values of $\mathbf{z}_1, \mathbf{z}_2, \mathbf{z}_3$ were computed, respectively, as follows: 0.5424, 0.0046, 0.0017 (the passive suspension); 0.5240, 0.0034, 0.0016 (the active suspension with single measurement); 0.5234, 0.0034, 0.0016 (the active suspension with two measurements).

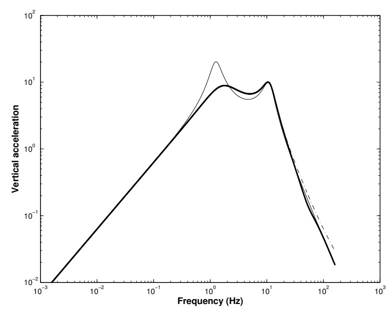

Fig. 3. The acceleration frequency response magnitude: $-$ Passive suspension; ... active suspension using the suspension travel measurement without tire damping; $-.$ active suspension using the acceleration and the suspension travel measurements without tire damping.

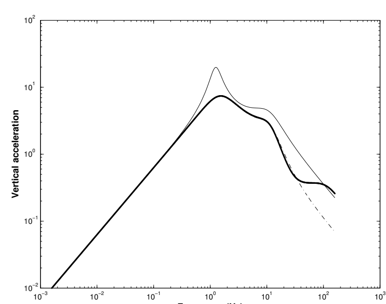

Fig. 4. The acceleration frequency response magnitude: $-$ Passive suspension; ... active suspension using the suspension travel measurement with tire damping $c_t = 2c_s$; $-.$ active suspension using the acceleration and the suspension travel measurements with tire damping $c_t = 2c_s$.

The natural frequency and the damping ratio of the heave mode are computed as $w_\mathrm{n}^\mathrm{h} = 1.2507$ Hz and $\zeta_1^\mathrm{h} = 0.2178$ for the passive suspension. For the wheel-hop mode, they are computed as $w_\mathrm{n}^\mathrm{wh} = 11.0247$ Hz and $\zeta_1^\mathrm{wh} = 0.2013$. The

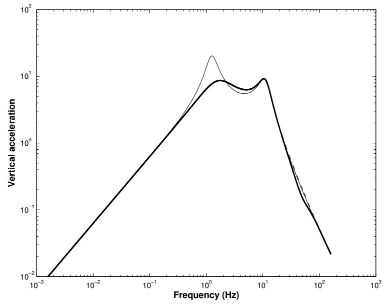

Fig. 5. The acceleration frequency response magnitude: $-$ Passive suspension; $\ldots$ active suspension using the suspension travel measurement with tire damping $c_t = 0.1c_s$; $-.$ active suspension using the acceleration and the suspension travel measurements with tire damping $c_t = 0.1c_s$.

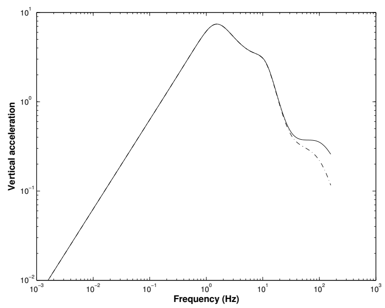

Fig. 6. The acceleration frequency response magnitude: $-$ Active suspension using the suspension travel measurement with the (fictitious) tire damping $c_t = 2c_s$; $-.$ active suspension designed by a mixture of the LQG methodology and the interpolation approach using the suspension travel measurement with the (actual) tire damping $c_t = 0.1c_s$.

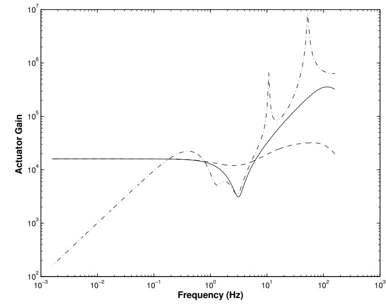

Fig. 7. The actuator frequency response magnitude using the suspension travel measurement: $-$ the LQG design with tire damping $c_t = 2c_s$; $--$ the LQG design with tire damping $c_t = 2c_s$; $-.$ the hybrid algorithm with tire damping $c_t = 0.1c_s$.

invariant frequencies are calculated from (7) as $\omega_1 = 3.832$ Hz and $\omega_2 = 10.610$ Hz. Since $\omega_2 \approx w_{\mathrm{n}}^{\mathrm{wh}}$, it is difficult to control the wheel-hop mode as clearly seen from Fig. 3. The 3.5 % drop in the rms vertical acceleration comes from the suppression of the heave mode vibration.

Now, let $c_{\mathrm{t}} = 2c_{\mathrm{s}}$. This value is unrealistic for tire damping because it yields $w_{\mathrm{n}}^{\mathrm{h}} = 1.2463$ Hz, $\zeta_1^{\mathrm{h}} = 0.2211$; $w_{\mathrm{n}}^{\mathrm{wh}} = 11.0628$ Hz, and $\zeta_1^{\mathrm{wh}} = 0.5919$. If c_{t} is set to $0.1c_{\mathrm{s}}$, then $w_{\mathrm{n}}^{\mathrm{h}} = 1.2504$ Hz, $\zeta_1^{\mathrm{h}} = 0.2180$; $w_{\mathrm{n}}^{\mathrm{wh}} = 11.0267$ Hz, and $\zeta_1^{\mathrm{wh}} = 0.2209$. Hence, the latter seems to be a realistic assumption. In Fig. 4, the counter part of Fig. 3 for the same values of the vehicle and the control design parameters but $c_{\mathrm{t}} = 2c_{\mathrm{s}}$ is plotted. Clearly, the response has been improved due to the removal of the invariant frequency at ω_2. For the rms values of $\mathbf{z}_1, \mathbf{z}_2, \mathbf{z}_3$, the following were respectively computed: 0.4513, 0.0043, 0.0011 (the passive suspension); 0.2834, 0.0036, 0.0010 (the active suspension with single measurement); 0.2724, 0.0037, 0.0010 (the active suspension with two measurements). Comparison of Fig. 4 with Fig. 3, and the modal natural frequencies and the damping ratios show that the improved responses are achieved by suppressing the wheel-hop vibration.

In Fig. 5 the vertical acceleration frequency response magnitude is plotted for the case $c_{\mathrm{t}} = 0.1c_{\mathrm{s}}$. The rms values for this case are, respectively, 0.5259, 0.0045, 0.0017 (the passive suspension); 0.4895, 0.0034, 0.0016 (the active suspension with single measurement); 0.4900, 0.0034, 0.0016 (the active suspension with two measurements). The rms vertical acceleration is reduced by 6.83 % which is about twice of the reduction computed for the case $c_{\mathrm{t}} = 0$. The rest of this section will be devoted to further enhancement of the closed-loop performance by means of the interpolation approach of this paper.

Put $c_t = \alpha c_s$ $(\alpha > 0)$ and $\mathbf{H}_{\mathrm{k}}(s;\alpha,\widehat{\mathbf{Q}}) = \mathbf{T}_{\mathbf{z}_{\mathrm{k}}\mathrm{v}_{\mathrm{i}}}$, $k = 1,2,3$ where $\widehat{\mathbf{Q}} = 1 - \mathbf{Q}$ and $\mathbf{Q} \in \mathscr{RH}_\infty$. Let $\alpha_1 = 0.1$, $\alpha_2 = 2$, and $\mathbf{Q}^\dagger$ and $\mathbf{Q}^\sharp$ denote the $\widehat{\mathbf{Q}}$ parameters of the compensators designed by the above LQG methodology with $c_t = \alpha_1 c_s$ and $c_t = \alpha_2 c_s$, respectively. As far as the closed-loop performance is concerned, $\mathbf{H}_{\mathrm{k}}(s;\alpha_2,\mathbf{Q}^\sharp)$, $k = 1,2,3$ are satisfactory while $\mathbf{H}_{\mathrm{k}}(s;\alpha_1,\mathbf{Q}^\dagger)$ are not. Thus, the interpolation problem to be studied:

Does there exist a $\widehat{\mathbf{Q}} \in \mathscr{RH}_\infty$ satisfying the equation: $\mathbf{H}_1(s;\alpha_1,\widehat{\mathbf{Q}}) = \mathbf{H}_1(s;\alpha_2,\mathbf{Q}^\sharp)$?

If there exists a solution to this problem denoted by $\widehat{\mathbf{Q}}$, then the quarter-car model in Fig. 1 with $c_t = 0.1c_s$ will have the closed-loop responses $\mathbf{H}_{\mathrm{k}}(s;2c_s,\mathbf{Q}^\sharp)$, $k = 1,2,3$ using the unique controller $\mathbf{K}$ corresponding to this $\widehat{\mathbf{Q}}$. Unfortunately, the formulated problem has no solution. To see this, first obtain the complete interpolation conditions for $\mathbf{T}_{\mathbf{z}_1\mathrm{v}_{\mathrm{i}}}$ as follows

1) $\mathbf{H}_1(s) = \dfrac{c_{\mathrm{s}}c_{\mathrm{t}}}{m_{\mathrm{s}}m_{\mathrm{u}}}s^{-1} + O(s^{-2})$,
2) $\mathbf{H}_1(0) = \mathbf{H}_1''(0) = 0, \qquad \mathbf{H}_1'(0) = 1.$

Then, from the first interpolation condition above

$$s\mathbf{H}_1(s;\alpha_1,\widehat{\mathbf{Q}})|_{s=\infty} = s\mathbf{H}_1(s;\alpha_2\mathbf{Q}^\sharp)|_\infty$$

which forces α_1 equal to α_2; hence, no solution. Having seen the infeasibility of this interpolation problem, consider now the following variant:

Does there exist a $\widehat{\mathbf{Q}} \in \mathscr{RH}_\infty$ satisfying the equation: $\mathbf{H}_1(s;\alpha_1,\widehat{\mathbf{Q}}) = \mathbf{H}_1(s;\alpha_2,\mathbf{Q}^\sharp)\Psi(s)$ for some $\Psi \in \mathscr{R}H_\infty$?

Fortunately, there exists a solution to the latter problem. In fact, from the interpolation conditions for $\mathbf{T}_{\mathbf{z}_1\mathrm{v}_{\mathrm{i}}}$, it suffices to pick any $\Psi \in \mathscr{RH}_\infty$ satisfying

1) $\Psi(0)=1$,
2) $\Psi'(0)=0$,
3) $\Psi(\infty)=\alpha_1/\alpha_2$.

It is easy to see that the following transfer function

$$\Psi(s)=\frac{\sigma s^2+as+b}{s^2+as+b}, \qquad a,b>0$$

where $\sigma=\alpha_1/\alpha_2$ has the aforementioned properties. Furthermore, for a given Ω which is sufficiently larger than the wheel-hop frequency $\omega_{\rm n}^{\rm wh}$, if a and b are chosen so that $\Psi(j\omega)$ is a good approximation the low-pass filter:

$$L_\Omega(\omega)=\begin{cases}1, & 0\le\omega\le\Omega,\\ \sigma, & \omega>\Omega\end{cases}$$

on the band $[0,\Omega]$, then a good match to the vertical acceleration response plotted in Fig. 6 is obtained. From the continuity of the trade-off curves, the rest of the responses are also seen to be satisfactory.

The free parameter $\widehat{\mathbf{Q}}$ is obtained with $\Delta(s;\alpha_1)$ calculated for $c_t=\alpha_1 c_s$. Since the degree of $\mathbf{H}_1(s;\alpha_2,\mathbf{Q}^\sharp)$ is 8, the degree of $\widehat{\mathbf{Q}}(s)$ is bounded above by 13. Finally, $\mathbf{K}$ is calculated by substituting $\mathbf{Q}=1-\widehat{\mathbf{Q}}$.

In Fig. 6, the acceleration frequency response magnitude of the active suspension designed by using the suspension travel measurement with the (fictitious) tire damping $c_t=2c_s$ plotted in Fig. 4 is reproduced along with the acceleration frequency response magnitude of the active suspension designed by the hybrid algorithm outlined above. The purpose of plotting them together was to show that the approximation $\mathbf{H}_1(s;\alpha_1,\widehat{\mathbf{Q}})\approx\mathbf{H}_1(s;\alpha_2,\mathbf{Q}^\sharp)$ is very accurate in the bandwidth of interest. A comparison of Fig. 5 with Fig. 6 reveals impressive closed-loop performance enhancement by the interpolation approach. In the simulation, $\psi(s)$ was chosen as

$$\psi(s)=\frac{0.05s^2+500s+10}{s^2+500s+10}.$$

In Fig. 7, the actuator frequency response magnitudes of the active suspensions designed by the LOG methodology with tire dampings $c_t=0.1c_s$ and $c_t=2c_s$, and the hybrid algorithm with tire damping $c_t=0.1c_s$ using the suspension travel measurement are plotted. Fig. 7 shows that the closed-loop performance enhancement by the interpolation approach is achieved at a reasonable price. Simulations for different values of tire damping have also been carried out. The numerical results have been observed to be insentive to changes in tire damping; hence confirming the predication about the efficency of coupling between the motions of the sprung and unsprung masses.

The rest of the paper will be devoted to a study of the rms performance limitations of the quarter-car models.

VI. Achievable rms responses

In this section, achievable rms responses of the quarter-car model to white-noise velocity road inputs will be parameterized. We assume that the derivative of w denoted by V_i obeys the relation in (8). Note that

$$\begin{aligned}\mathbf{T}_{\mathbf{z}V_i} &= -\frac{s}{\Delta}\begin{bmatrix}-(\mathrm{c_t}s+\mathrm{k_t})(\mathrm{c_s}s+\mathrm{k_s})\\ \mathrm{m_s}(\mathrm{c_t}s+\mathrm{k_t})\\ \mathrm{m_s}\mathrm{m_u}s^2+(\mathrm{m_s}+\mathrm{m_u})\mathrm{c_s}s+(\mathrm{m_s}+\mathrm{m_u})\mathrm{k_s}\end{bmatrix}\\ &\quad+\frac{\mathrm{m_s}s(\mathrm{c_t}s+\mathrm{k_t})}{\Delta^2}\begin{bmatrix}s^2[\mathrm{m_u}s^2+\mathrm{c_t}s+\mathrm{k_t}]\\ (\mathrm{m_s}+\mathrm{m_u})s^2+\mathrm{c_t}s+\mathrm{k_t}\\ -\mathrm{m_s}s^2\end{bmatrix}Q.\end{aligned}$$

The autocovariance function of $\mathbf{z}$ is calculated from (8) as

$$\mathbf{R_z}(\tau)=2\pi n_0^2\kappa v\int_{-\infty}^{\infty}\mathbf{T}_{\mathbf{z}V_i}(j\omega)\mathbf{T}_{\mathbf{z}V_i}^{\sim}(j\omega)e^{-j\omega\tau}\,d\omega \qquad (9)$$

where $H^\sim(s)=H^T(-s)$. The square roots of the elements in the diagonal of $\mathbf{R_z}(0)$ equal to the rms values of the vertical acceleration, the suspension travel, and the tire deflection. Note from (9) that the sum of the diagonal elements of $\mathbf{R_z}(0)$ is given by

$$J(Q)=(2\pi n_0)^2\kappa v\|\mathbf{T}_{\mathbf{z}V_i}\|_2^2. \qquad (10)$$

We will consider weighted and optimized version of (10):

$$J^*(\Lambda)=(2\pi n_0)^2\kappa v\inf_{Q\in\mathscr{R}H_\infty}\|\Lambda\mathbf{T}_{\mathbf{z}V_i}\|_2^2 \qquad (11)$$

where Λ is a diagonal matrix with nonnegative entries $\lambda_1,\lambda_2,\lambda_3$. Letting $\mathrm{E}(x)$ denote the expected value of a given random variable x, we see that the control input chosen in (11) mimimizes $\sum_{k=1}^3\lambda_k^2\,\mathrm{E}[\mathbf{z}_k^2]$ with respect to the set of all stabilizing controllers.

VII. Root–mean–square performance limitations

Let

$$\begin{aligned}\mathbf{F} &= -\frac{s\Lambda}{\Delta}\begin{bmatrix}-(\mathrm{c_t}s+\mathrm{k_t})(\mathrm{c_s}s+\mathrm{k_s})\\ \mathrm{m_s}(\mathrm{c_t}s+\mathrm{k_t})\\ \mathrm{m_s}\mathrm{m_u}s^2+(\mathrm{m_s}+\mathrm{m_u})\mathrm{c_s}s+(\mathrm{m_s}+\mathrm{m_u})\mathrm{k_s}\end{bmatrix},\\ \mathbf{H} &= \frac{\Lambda}{\Delta}\begin{bmatrix}s^2[\mathrm{m_u}s^2+\mathrm{c_t}s+\mathrm{k_t}]\\ (\mathrm{m_s}+\mathrm{m_u})s^2+\mathrm{c_t}s+\mathrm{k_t}\\ -\mathrm{m_s}s^2\end{bmatrix}\end{aligned}$$

and assume that $\Lambda\in\mathbf{R}^{3\times3}$ is nonsingular. From (11),

$$J^*(\Lambda)=(2\pi n_0)^2\kappa v\inf_{Q\in\mathscr{R}H_\infty}\|\mathbf{F}-\mathrm{m_s}s(\mathrm{c_t}s+\mathrm{k_t})\Delta^{-1}\mathbf{H}Q\|_2^2.$$

Since $\mathbf{H}$ has full rank on the imaginary axis including ∞ and $\mathrm{m_s}s(\mathrm{c_t}s+\mathrm{k_t})\Delta^{-1}$ has no zeros in the open right half plane, Lemma 6.3.10 in [11] can be applied. Thus,

$$J^*(\Lambda)=(2\pi n_0)^2\kappa v\inf_{Q\in\mathscr{R}H_\infty}\|\mathbf{F}-\mathbf{H}Q\|_2^2.$$

Next, an inner-outer factorization of $\mathbf{H}$ is done. In doing so, first get a spectral factor of $\mathbf{H}^\sim(s)\mathbf{H}(s)$. If the quadruplet $(\mathbf{A},\mathbf{B},\mathbf{C},\mathbf{D})$ denotes a minimal state-space realization of $\mathbf{H}(s)$, then a spectral factor denoted by $H_{\rm o}(s)$ is given by

$$H_{\rm o}(s)=\left(\mathbf{A},\mathbf{B},\underline{D}^{-\frac12}(\mathbf{D}^T\mathbf{C}+\mathbf{B}^T\mathbf{X}),\underline{D}^{\frac12}\right)$$

where $\underline{D}=\mathbf{D}^T\mathbf{D}$ and $\mathbf{X}$ is the stabilizing solution of the Riccati equation:

$$\begin{aligned}(\mathbf{A}-\mathbf{B}\underline{D}^{-1}\mathbf{D}^T\mathbf{C})^T\mathbf{X} &+ \mathbf{X}(\mathbf{A}-\mathbf{B}\underline{D}^{-1}\mathbf{D}^T\mathbf{C})-\mathbf{X}\mathbf{B}\underline{D}^{-1}\mathbf{B}^T\mathbf{X}\\ &+ \mathbf{C}^T(I-\mathbf{D}\underline{D}^{-1}\mathbf{D}^T)\mathbf{C}=0.\end{aligned}$$

The inner factor is then

$$\mathbf{H}_{\rm i}(s) = \mathbf{H}(s)H_{\rm o}^{-1}(s).$$

The next step is the calculation of a complementary inner factor $\mathbf{N}_\perp$ of $\mathbf{H}_{\rm i}$, *i.e.,* finding a matrix $\mathbf{N}_\perp$ that makes $[\mathbf{H}_{\rm i}\ \mathbf{N}_\perp]$ square and inner. If $(\mathbf{A}_1, \mathbf{B}_1, \mathbf{C}_1, \mathbf{D}_1)$ is a minimal state-space realization of $\mathbf{H}_{\rm i}$, then a realization of $\mathbf{N}_\perp$ is given by the formula [12][Lemma 13.31]:

$$\mathbf{N}_\perp = \left(\mathbf{A}_1, -\mathbf{Y}^{-1}\mathbf{C}_1^T\mathbf{D}_\perp, \mathbf{C}_1, \mathbf{D}_\perp\right)$$

where $\mathbf{D}_\perp$ is an orthogonal complement of $\mathbf{D}_1$ such that $[\mathbf{D}_1\ \mathbf{D}_\perp]$ is square and orthogonal and $\mathbf{Y}$ is the observability Gramian:

$$\mathbf{A}_1^T\mathbf{Y} + \mathbf{Y}\mathbf{A}_1 + \mathbf{C}_1^T\mathbf{C}_1 = 0.$$

Observe that $\mathbf{H}_{\rm i}$ and $\mathbf{N}_\perp$ have four common poles. Note that $H^T(\infty) = (\lambda_1/m_{\rm s}, 0, 0)$. Thus, $\mathbf{D}_\perp$ can be chosen as

$$\mathbf{D}_\perp = \begin{bmatrix} 0 & 0 \\ 1 & 0 \\ 0 & 1 \end{bmatrix}.$$

Let $\mathscr{H}_2$ denote the Hilbert space of complex functions that are analytic on the open right half plane and let $\mathscr{H}_2^\perp$ be its complement in $\mathscr{L}_2$, the set of complex functions which are square integrable on the imaginary axis. Let Π and $\Pi^\perp$ denote respectively the orthogonal projections from $\mathscr{L}_2$ onto $\mathscr{H}_2$ and $\mathscr{H}_2^\perp$. Then,

$$\inf_{Q\in\mathscr{R}H_\infty} \|\mathbf{F} - \mathbf{H}Q\|_2^2 \quad = \quad \|\mathbf{N}_\perp^\sim\mathbf{F}\|_2^2 + \|\Pi^\perp\mathbf{H}_{\rm i}^\sim\mathbf{F}\|_2^2$$

with

$$Q = H_{\rm o}^{-1}\Pi\mathbf{H}_{\rm i}^\sim\mathbf{F}. \tag{12}$$

Hence,

$$J^*(\Lambda) = (2\pi n_0)^2\kappa v\left\{\|\Pi\mathbf{N}_\perp^\sim\mathbf{F}\|_2^2 + \|\Pi^\perp\mathbf{N}_\perp^\sim\mathbf{F}\|_2^2 + \|\Pi^\perp\mathbf{H}_{\rm i}^\sim\mathbf{F}\|_2^2\right\}.$$

Note that Q in (12) is only an approximitation to the Q-parameter of the optimal controller. If w is not an integrated white-noise process; but its derivate is a colored-noise process, *i.e.,* $V_{\rm i} = \dot{w} = \Psi\eta$ for some linear shape filter $\Psi \in \mathscr{R}H_\infty$ with $\Psi^{-1} \in \mathscr{R}H_\infty$, the whole argument above is the same provided that $\mathbf{F}$ is replaced with $\mathbf{F}\Psi$.

Finally, we investigate the effect of tire damping on the optimal cost $J^*(\Lambda)$ for a given nonnegative diagonal weight matrix Λ. We fix Λ as $\mathrm{diag}(1,1,1)$. It will be more convenient to define a dimensionless quantity:

$$\mu(c_{\rm t}) = \frac{[J^*(\mathrm{diag}(1,1,1))]^{1/2}}{[J(0)]^{1/2}}.$$

Thus, $\mu(c_{\rm t})$ is a measure of active suspension performance relative to the passive suspension performance in the root–mean–square sense. In Fig. 8, $\mu(c_{\rm t})$ is plotted versus $c_{\rm t}$. Tire damping remarkably improves the closed-loop performance as predicated by the theory.

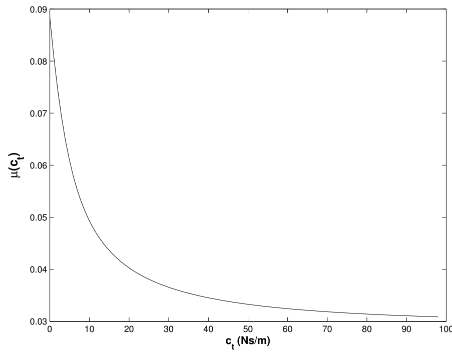

Fig. 8. Optimized performance index scaled by the open-loop performance index as a function of tire damping coefficient.

VIII. CONCLUSIONS

In this paper, performance limitations were studied for a quarter-car active suspension system excited by sinusoidal or random road disturbances. It was demonstrated that the influence of tire damping on the closed-loop performance of the active suspension system can be significant.

REFERENCES

[1] D. Karnopp, Active and semi-active vibration isolation, *Transactions of the ASME, J. Mechanical Design* 117 B (1995) 177–185.

[2] D. Hrovat, Survey of advanced suspension developments and related optimal control applications, *Automatica* 33 (1997) 1781–1817.

[3] C. Yue, T. Butsuen, and J. K. Hedrick, Alternative control laws for automotive active suspensions, *Transactions of the ASME, J. Dynamic Systems, Measurement, and Control* 111 (1989) 286–291.

[4] J. K. Hedrick and T. Butsuen, Invariant properties of automotive suspensions, In: *Proc. Inst. Mech. Engineers, Part D, Transport Engineering* 204 (1990) 21–27.

[5] D. Karnopp, Theoretical limitations in active suspensions, *Vehicle System Dynamics* 15 (1986) 41–54.

[6] M. C. Smith, Achievable dynamic response for automotive active suspensions, *Vehicle System Dynamics* 24 (1995) 1–34.

[7] M. C. Smith and G. W. Walker, Performance limitations and constraints for active and passive suspensions: A mechanical multi-port approach, *Vehicle System Dynamics* 33 (2000) 137–168.

[8] S. Türkay and H. Akçay, Aspects of achievable performance for quarter-car active suspensions, *J. Sound & Vibr.* 311 (2007) 440-460.

[9] J. A. Levitt and N. G. Zorka, Influence of tire damping in quarter car active suspension models, *Trans. ASME, Journal of Dynamic Systems, Measurement, and Control* 113 (1991) 134–137.

[10] Dodds, C. J. and Robson, J. D., The description of road surface roughness, *J. Sound & Vibr.*, 2, 175–183, 1973.

[11] M. Vidyasagar, *Control System Synthesis: A Factorization Approach*, Cambridge, Massachusetts: MIT Press, 1985.

[12] K. Zhou, J. C. Doyle, and K. Glover, *Robust and Optimal Control*, Prentice-Hall, Upper Saddle River,1996.